DEVELOPMENT OF HIGH-LIFT SYSTEMS FOR THE BOMBARDIER CRJ-700

Fassi Kafyeke, François Pépin and Cedric Kho
Advanced Aerodynamics, Bombardier Aerospace
Montréal, Canada

Keywords: *flaps, slats, high-lift, wind tunnel testing*

Abstract

This paper describes the development process of the low-speed configuration of the CRJ-700, with an emphasis on half-model high Reynolds number wind tunnel testing. The process included CFD design and analysis, wind tunnel tests and flight tests. The experimental development of the flaps and slats was performed using a 7% scale half-model, in the IAR 5ft x5ft High Reynolds Number wind tunnel. Results from these tests are in very good agreement with flight test data and decisions made in the wind tunnel lead to a short and successful flight test program.

1 Introduction

Over the last decade, Bombardier Aerospace designed and put into production a number of regional and business aircraft. The CRJ-700 is a 70-seat version of the highly successful Canadair Regional Jet CRJ-200. The CRJ-700 wing was essentially a blank sheet design with a completely new planform and with the addition of leading edge devices. During the development of the CRJ-700 aerodynamic configuration, the low-speed characteristics of the airplane were carefully studied. Three considerations guided the design: safety, simplicity and performance. In practice, safety required clearly identifiable stall characteristics with a nose down pitching moment and little or no roll excursion. For simplicity, double-slotted hinged flaps similar to those of the CRJ-200 were used. Performance meant as much usable lift as possible and good second-segment-climb capability.

2 Aircraft Design Characteristics

The CRJ-700 was designed to carry seventy passengers and three crew members over a range of 1685 Nautical Miles (1985 NM for the extended range version) at Mach number 0.78. Maximum operating Mach number is 0.83 and maximum cruising altitude 41,000 feet. The aircraft, designed with a Maximum Take-Off Weight (MTOW) of 73,000 lbs (75,250 lbs for the extended range version), is powered by two fuselage mounted General Electric CF-34-8C1 turbofans, each developing 12,670 lbs thrust. The take-off distance at MTOW is 5,130 ft and the landing distance, at the Maximum Landing Weight of 67,000 lbs is 4850 ft. Figure 1 gives the general arrangement of the aircraft.
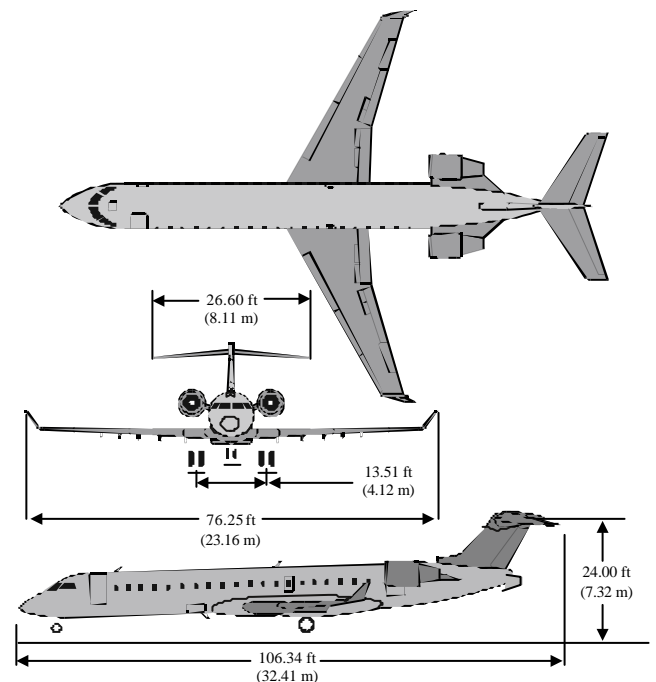

Figure 1: CRJ-700 aircraft general arrangement

3 CRJ-700 High Lift Wing Design

3.1 Planform Design

The CRJ-700 initial wing planform W30 was obtained from the CRJ-200 wing by adding a 72" root plug and extending the leading edge by 9% chord (Figure 2). The intention was to maintain the existing wing box structure on the outer wing panel and limit airfoil modifications to the part of the wing forward of the front spar. This planform was abandoned after it was realized that the resulting wing sections could not provide adequate high-lift characteristics. The leading edge crank was also an impediment to the installation of a simple leading edge device. A new planform, W33, was designed, with the 72" root plug but this time with a straight leading edge. The constraint of preserving the CRJ-200 front spar was also removed and new advanced supercritical wing sections were designed. The wing retained the simple double-slotted hinged flaps in two segments of the CRJ-200 and was fitted with new leading edge slats. After the first series of high speed and low speed tests, the W33 wing was replaced by wing W34, with the same planform and improved wing sections. Flaps and slats were redesigned to accommodate the new wing geometry.
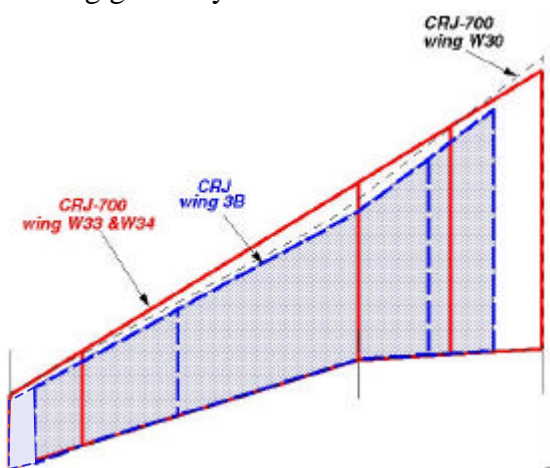
Figure 2: CRJ-700 wing planform development

The reference area of wing W34 is 738 ft^2 and its aspect ratio 7.38. The quarter chord sweep of the outboard wing panel is 26.9 degrees. The wing is fitted with winglets canted 20 degrees.

3.2 High Lift System Design

Figure 3 shows the planform definition of the CRJ-700 high-lift system. The trailing edge flaps are double-slotted hinged flaps. The inboard flap has a constant 33-inch chord and is fitted with a spring-loaded constant chord flap vane. The outboard flap is physically the same as the outboard flap of the CRJ-200. The flap chord is a constant percentage of the main wing chord (24% chord). It is fitted with a fixed tapered flap vane. The inboard flap deflection angles are 10 and 20 degrees for take-off, 30 degrees for approach and 45 degrees for landing. The outboard flap is geared with a ratio 8/9 to the inboard flap deflections, deploying therefore to 40 degrees in landing. The gearing improves the spanwise load and preserves excellent aileron performance in all configurations. The leading edge slats cover the full span except for an inboard segment of the wing, which was left unprotected to improve the stall characteristics. The slats are tapered, covering 15% of the wing chord at the break and 17% chord at the wing tip. The slat deflections are 20 degrees for 0 and 10 degrees flap settings and 25 degrees for all other flap settings.
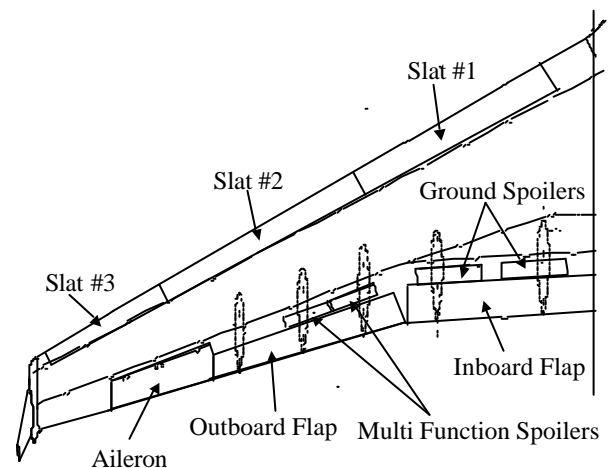
Figure 3: CRJ-700 flaps and slats planform definition

Two pairs of multifunction spoilers supplement the ailerons and two pairs of ground spoilers complete the set of wing movable surfaces. The trailing edge flaps of the CRJ-700 retain the simplicity of the CRJ-200 design. Figure 4 shows various settings of the inboard flap. The

flap rotates around a fixed hinge axis to 45 degrees. A small vane is nested against the flap leading edge in the flap-retracted position and springs into position as the flap is deployed. The vane on the outboard flap (Figure 5) is fixed to the flap. This outboard flap rotates to 40 degrees, in a geared ratio to the inboard flap setting. A bent up trailing edge (BUTE) door improves the flow in the cove region on the outboard flap. At flap deflections below 20 degrees, the BUTE door effectively seals the passage to the upper surface of the vane, allowing the flap to operate as a single-slotted flap. This improves the lift to drag ratio of the take-off configuration.
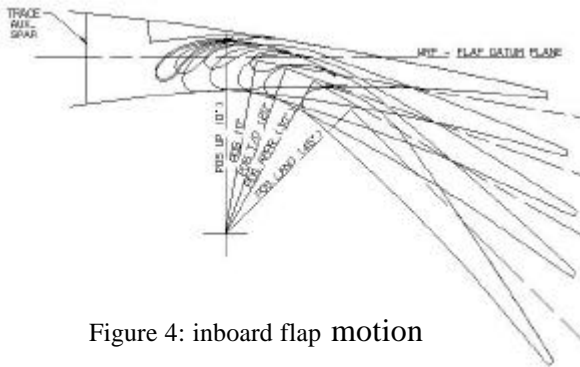

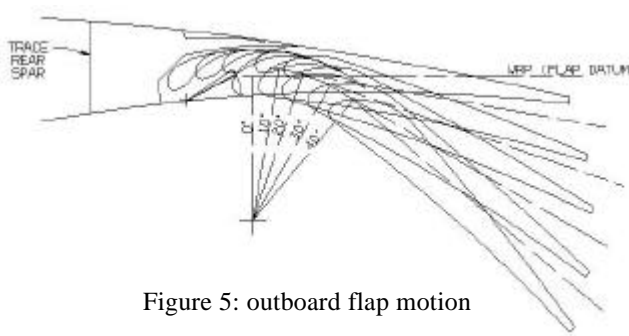Figure 4: inboard flap motion

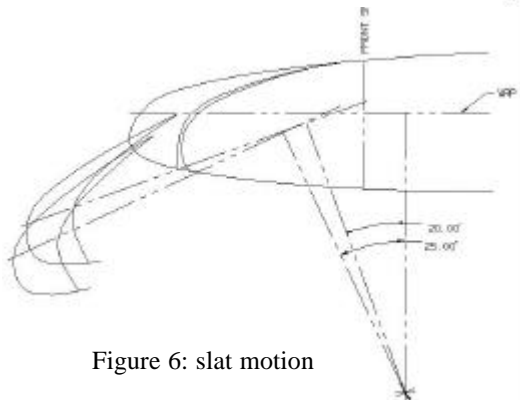Figure 5: outboard flap motion

Figure 6: slat motion

Figure 6 illustrates the slat settings. For simplicity, the slats are deployed along a circular arc track with three positions: retracted,

20 degrees for normal take-off and 25 degrees for short take-off, approach and landing.

4 Theoretical Methods

At the early stages, the development of the high-lift systems was conducted using Computational Fluid Dynamics (CFD) methods: three codes were used for the design of the multi-element airfoils. CEBECI, a viscous panel method with strong boundary layer coupling developed by T. Cebeci and his team at the University of California in Long Beach [1], was used for rapid evaluation of configurations. The MSES viscous Euler code of Drela [2] and the NSU2D 2D unstructured grid Navier-Stokes code developed by D. Mavriplis [3] were used for the design and final verification of flaps and slats.
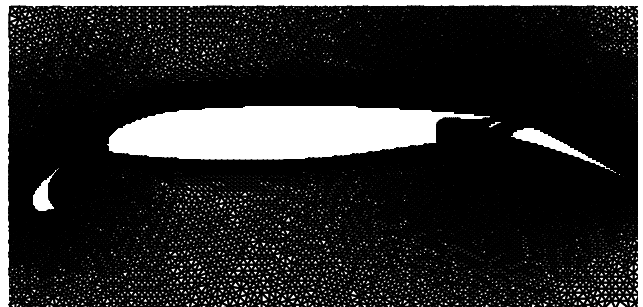

Figure 7: NSU2D unstructured Navier-Stokes grid for a CRJ-700 multi-element airfoil.

The accuracy of these codes for high-lift computations was verified in a two-dimensional high Reynolds number high-lift test that was carried out on a Bombardier generic multi-element airfoil in the IAR 2D test facility in Ottawa [4]. In Figure 8, pressure distributions obtained with the NSU2D Navier-Stokes code and the CEBECI2D viscous panel method are compared. Some of the differences may be due to different transition settings between the two codes. The Navier-Stokes solution is a fully turbulent one, whereas natural transition locations are predicted, using semi-empirical criteria, in the viscous panel code. The 3D high-lift characteristics were predicted using the Analytical Methods Inc.'s VSAERO 3D panel method and Bombardier's semi-empirical stall prediction methods developed and validated on the Challenger CL-604, the CRJ-200 and the

Global Express. This method is based on the criterion proposed by Valarezo [5]. Figure 9 shows a typical VSAERO solution. Figure 10 shows the predicted C_{Lmax} for the clean configuration in wind tunnel conditions, compared to the experimental data.
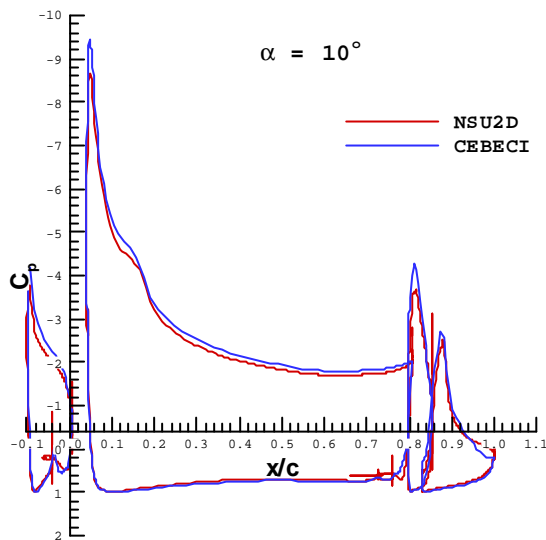

Figure 8: Pressure distributions computed with the CEBECI and NSU2D codes on a CRJ-700 section; slat 28 degrees, flap 40 degrees; M = 0.20, α=10 degrees, Re=12 Million.
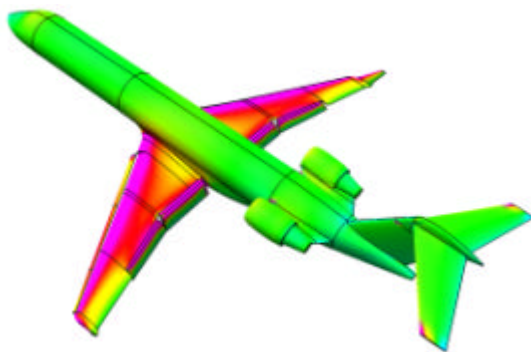

Figure 9: VSAERO solution for a CRJ-700 early landing configuration, flap setting: 45 degrees, slat setting: 28 degrees Mach 0.2, Alpha=10 degrees

5 Wind Tunnel Testing

The CFD design was further optimized in the wind tunnel. The low speed wind tunnel tests were conducted in three phases:

- Initial development wind tunnel tests to validate CFD designs and to obtain initial performance figures. These tests used the early wing configuration W33.
- Detailed design and development wind tunnel tests leading to the aerodynamic freeze of the external lines. These tests used the final wing configuration W34.
- Production wind tunnel tests to verify in detail many aircraft possible configurations and to obtain the data needed before the aircraft first flight. These tests used the production configuration of the aircraft.

Two low-speed tests were conducted in each phase: a high-Reynolds number half-model test and a low Reynolds number full model test.
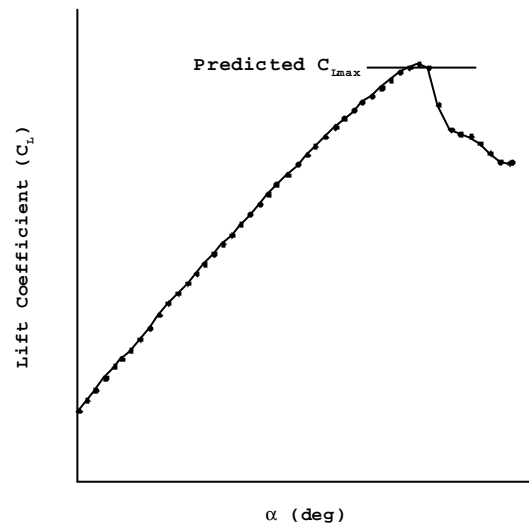

Figure 10: Comparison of wind tunnel data with theoretical prediction of CLmax for the CRJ-700 clean configuration at wind tunnel conditions: Mach 0.20, chord Reynolds number 6.5 million.

The first high-lift development test was conducted in January 1996 using a 7% scale half-model in the 5ft x 5ft wind tunnel of the Canadian Institute for Aerospace Research (IAR) in Ottawa. The objectives in this test were:

- to evaluate various flap and slat designs and establish optimal angles, gaps and overlaps;
- to determine the optimal location and geometry of the inboard slat inboard end;
- to measure C_{Lmax} and determine longitudinal stall characteristics;

- to investigate Mach number and Reynolds number effects;
- to measure the effectiveness of control surfaces in high-lift configurations at high Reynolds number.

Comparison with data obtained at lower Reynolds number in full model tests at the IAR 6ftx9ft atmospheric tunnel and at the MicroCraft 7ftx7ft high-speed tunnel in El Segundo, California, were used to estimate the half-model corrections.

The second high-lift development test was carried out in January 1997, using a configuration with the final wing W34. The objectives of the test were the same as those of the first phase, but with a view to freezing the high-lift systems. The test was also used to determine the final take-off and landing flap and slat settings, including alternate configurations and to establish the effect of various ice shapes on the wing and tailplane. Slat loads were measured using specially designed strain-gauged components.

5.1 Wind Tunnel Description

The IAR 5ft x 5ft tunnel is a blow-down facility, shown schematically in Figure 11, which can be used to test in the subsonic, transonic and supersonic flow regimes.
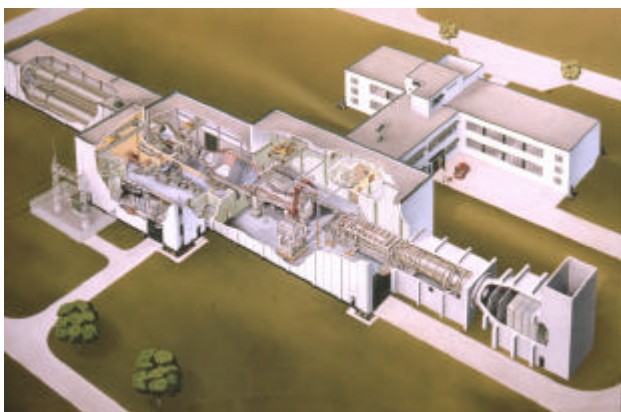

Figure 11: NRC/IAR High Reynolds number blow-down tunnel

The reflection plane model was installed in the 5-ft transonic test section with perforated walls as shown in Figure 12. The wall porosity was set at 4.0% open during the entire investigation.

The test section was configured for half-model testing with a solid 135.5-inch long and 0.25-inch thick reflection plate, with an elliptic leading edge, installed on stand-off from the north perforated wall.
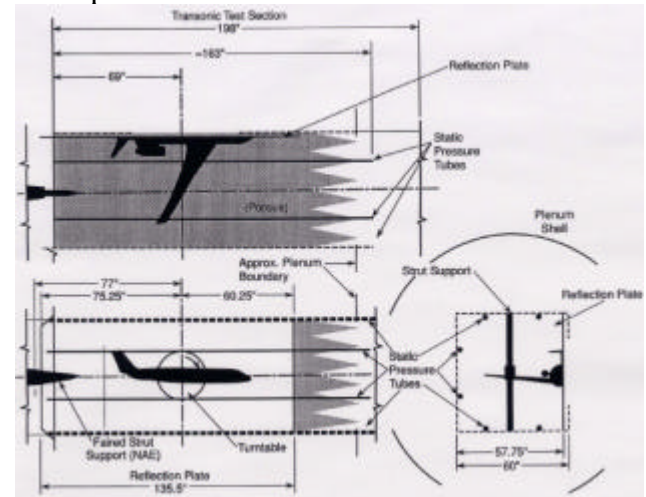

Figure 12: Wind tunnel half-model test section

A non-metric boundary layer plate was installed between the model and the reflection plate. The outboard of the plate was attached to a turntable and slaved to the balance rotation. The loads were measured with the IAR 5-component sidewall balance. The incidence of the model was measured using an accelerometer mounted in the fuselage center section. A potentiometer mounted on the half-model support system provided a secondary reading of the model incidence, which was used to control model pitching. A check calibration of both incidence measurements was made prior to the investigation and the incidence zero for both measurements established as part of the process. The instrumentation to establish the tunnel conditions was as follows: three 200-psi absolute pressure transducers were used to measure the settling chamber stagnation pressure, the tunnel static pressure (on the tunnel ceiling) and a "slugged volume" reference pressure. A 45-psi absolute pressure transducer was used to measure the atmospheric pressure. A resistance thermometer in the settling chamber measured the stagnation temperature. Model pressure measurements were performed using an Electronic Scanning Pressure (ESP) system using modules mounted

in the fuselage cavity. All pressures were measured relative to the "slug volume" reference pressure. Other modules connected to the ESP system were used to obtain the tunnel wall pressure signatures from six wall static tubes installed in the test section.

5.2 Model Description

The model was a 7% scale representation of the starboard half of the CRJ-700 aircraft, as shown in Figure 13. The reflection plane model was mounted to the tunnel sidewall balance through the use of an L-shaped bracket. A 1-inch thick boundary layer plate, identical in plan view to the perimeter of the aircraft plane of symmetry, isolated the model from the wall. There was a 0.1-inch spacing between the model plate and the boundary layer plate. A triple labyrinth seal on the outboard face of the boundary layer plate prevented dynamic pressure build up between the model plate and the boundary layer plate. A single electric contact was installed to indicate any labyrinth fouling under load.

Figure 13: 7 percent scale half-model of the CRJ-700 installed in the IAR 5-ft high Reynolds number wind tunnel

The gap between the reflection plate and the boundary layer plate was pneumatically sealed with Teflon strips. In addition, a rubber skirt was attached to the outer perimeter of the boundary layer plate as shown in Figure 14. The wing was made out of high tempered stainless steel. It was bolted to the L-shaped bracket. Conventional lap joints machined at the periphery of the wing bar accepted detachable

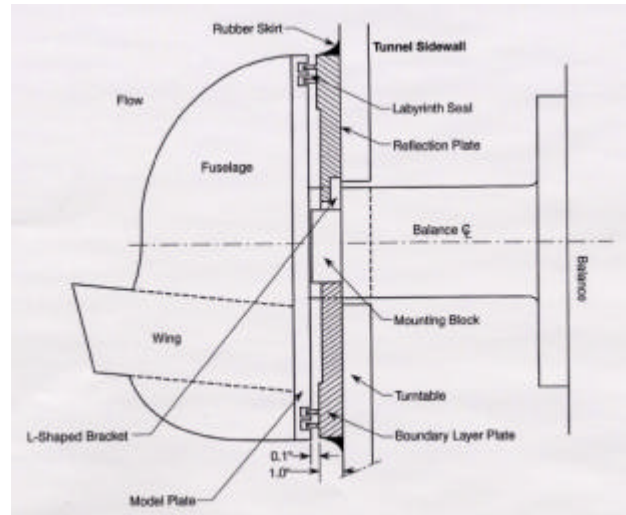clean wing leading and trailing edges or high-lift devices.

Figure 14: Schematic of the model mounting arrangement

A detachable winglet, BUTE doors and an assortment of control surfaces (ailerons, ground spoilers and multifunction spoilers) completed the list of wing components. The wing was instrumented with three rows of pressure taps oriented streamwise: the first one at the inboard flap mid-span, the second one at the outboard flap mid-span and the third one at the aileron mid-span. The tubes were all inside the wing and ran into conventional chordwise drilling and spanwise troughs towards the pressure scanners located inside the forward fuselage. The clean wing configuration was fitted with 111 pressure taps and the high-lift configuration with 192 pressure taps. The part-span steel leading edge slat was built in three sections representative of the aircraft arrangement. Three brackets per segment, representative of the real aircraft installation in their orientation and location, ran on fixed circular tracks inside the fixed wing under-slat surface (WUSS). Each slat segment was instrumented with two rows of taps oriented hingewise (normal to the front spar) for slat load measurements. Due to their large number, the rigid pressure tubes ran inside a dummy bracket replacing the middle slat bracket on each segment. An additional slat/WUSS assembly with three stain-gauged balances located inside the wing was

manufactured. These components were used to measure slat loads in selected runs.

The trailing edge flaps consisted of two double-slotted hinged flaps. As on the real airplane, the inboard flap was supported by two flap track fairings and the outboard flap by three flap track fairings. The two outer fairings of each flap incorporated a compass mechanism that was used to set all the required flap angles. A vane attached to each flap could be repositioned for gap and overlap investigation. The fuselage was bolted to the L-shaped bracket. It integrated the vertical stabilizer in order to attach the horizontal stabilizer. A pylon and a flow-through nacelle were attached to the fuselage. The nacelle was designed to represent the engine inlet mass flow at one idle operating condition. Electronic pressure scanners connected to the wing pressure ports and the model plate inboard taps were fitted inside the forward fuselage. The cantilevered horizontal tailplane could be indexed at all required incidences. The elevator, mounted on hinges, was deflected into position using brackets.

5.3 Test Procedures

Bombardier used this high Reynolds number facility for high-lift systems development for the first time during the Global-Express business jet project. Procedures leading to valid and repeatable forces, moments and pressure measurements were established then. The main challenge was to obtain stabilized flow qualities during a period sufficiently long to traverse the large range of angles of incidence required for high-lift experiments. Most of the CRJ-700 runs were performed at a nominal Mach number of 0.20 and a Reynolds number of 8.40 million per foot or 6.5 million based on the model reference chord. Additional runs were made at Mach 0.15, 0.30 and 0.40 to investigate Mach number effects. At Mach 0.20, runs were also made at three additional Reynolds numbers: 4.7, 7.3 and 10 million per foot to investigate scale effects. The model was pitched through a range of angles of incidence between –6 degrees and 25 degrees for non-slatted configurations and between –6 degrees and 30 degrees for

configurations with deployed slats. A few runs were made during which the model was pitched to 33.5 degrees. After examination of the repeatability of force and pressure data obtained with fixed pitch, pitch pause and continuous sweep runs, subsequent runs were made with continuous pitch motion at the slowest sweep rate compatible with available stable flow conditions. This time varied between 15 and 30 seconds, depending on the Mach number and Reynolds number selected [6]. The electronically collected data was filtered at 3 Hertz then digitized at 100 samples per second. The aerodynamic data was corrected for wind tunnel wall interference using the wall pressure signature. The correction was based on a procedure developed for half-models by Mokry [7]. The procedure uses the model geometry, the cross-sectional area distribution and the tunnel parameters. It yields corrections ΔM to the freestream Mach number, $\Delta\alpha$ to the model angle of incidence and $\Delta C_{Dbuyancy}$ to the drag. Corrections for the tunnel freestream flow angularity were applied to the data using pre-calibrated correction algorithms. All high Reynolds number high-lift runs were performed transition-free on the wing. Transition was fixed on all other surfaces using polyester-resin cylinders. A selected number of flow visualization runs were performed using the fluorescent mini-tuft technique. Repeatability on maximum lift coefficient was $\Delta C_{Lmax} = 0.01$ to 0.02 and the scatter on α_{stall} was negligible. Repeatability on the drag of high lift configurations was $\Delta C_D = 20$ to 30 drag counts. Measurements of pitching moments were repeatable within $\Delta C_M = 0.01$. With these values, the IAR 5-ft tunnel test was considered adequate for the validation of flaps and slats geometry and kinematics and the prediction of C_{Lmax} and global longitudinal stall characteristics. To predict tailplane angles to trim and the drag polars of take-off and landing configurations, it was necessary to resort to data from a 7% scale full model test performed at the IAR 6ftx9ft wind tunnel (Figure 15)
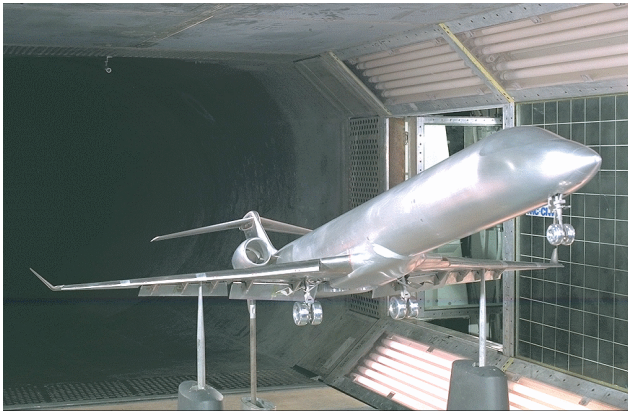
Figure 15: 7% scale full model of the CRJ-700 in IAR 6ft x 9ft atmospheric wind tunnel

5.4 Selected Wind Tunnel Test Results

In Figure 16, results obtained in the 5-ft tunnel on a tail-off half-model are compared with those obtained on a sting-mounted full model. Both results were obtained for the same Mach number (0.25), chord Reynolds number (2.8 Million) and the same transition trip configuration (wing tripped at 0.5% chord below the leading edge).
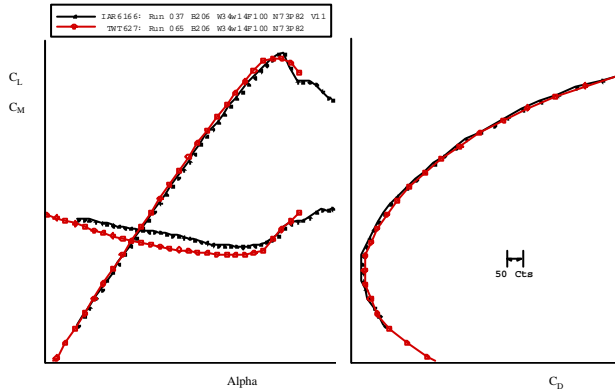

Figure 16: Half-Model effects; comparison of lift, drag and pitching moment coefficients on CRJ-700 tail-off configuration at Mach 0.25 Re_c=2.8 Million. Open symbols: full model, closed symbols: half-model

This figure shows a good correlation of lift and drag but a clear shift in pitching moment. Tests performed earlier on the Global Express had shown that this is due to a larger down force on the fuselage mounted nacelle and pylon on the half-model. Pitching moments measured on wing-body configurations are much closer. This, however, did not change the stall angle or the pattern of the stall on the wing. The high-lift tests showed that the redesigned airfoil sections on wing W34 had improved the clean

configuration C_{Lmax} by 0.04. Configurations investigated included flap angles 0, 10, 20,30 and 45 degrees. Slats were deflected along a simple circular arc track. The slat angles available were 15 degrees (sealed slats), 17, 20, 22, 25, 28 and 30 degrees (gapped slats). Decisions made on the basis of wind tunnel test data included: selection of optimum slat angles for take-off and landing; selection of a trim location for the inboard slat; extension of the slat chord at the wing tip from 15% chord to 17% chord. Investigation of Reynolds number effects on lift and drag was done to support extrapolation of wind tunnel test data to full scale.

Figure 17 shows the lift and pitching moment characteristics with various trim locations of the inboard end of the inboard slat: "sl1b" is the full span slat, "sl2b" an intermediate trim location and "sl3b" the most outboard trim location considered. This figure shows C_{Lmax} reducing as more of the leading edge is left unprotected. The benefit is improved pitching moment characteristics at stall.
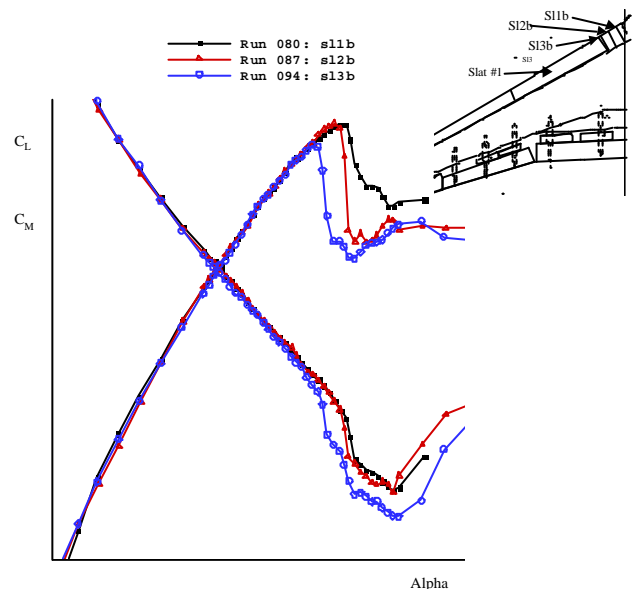

Figure 17: Effect of varying the location of the inboard slat trim on CRJ-700 configuration; Mach 0.20 Rec=6.5 Million. Flaps 45 degrees, slats 28 degrees; it=-9 degrees.

The depth of the pitching moment "bucket" occurring at stall represents the extent of flow

separation on the inboard wing. The width of the bucket indicates the angle of incidence margin between the initial inboard flow separation and flow separation on outer parts of the wing. Selection the "sl3b" trim location for the aircraft effectively meant trading off some C_{Lmax} for better stall characteristics.

A decision was also made to extend the slat chord at the wing tip from 15% of the wing chord to 17% chord. Figure 18 shows the effect of this extension on the high-lift characteristics of a landing configuration with the tail off.
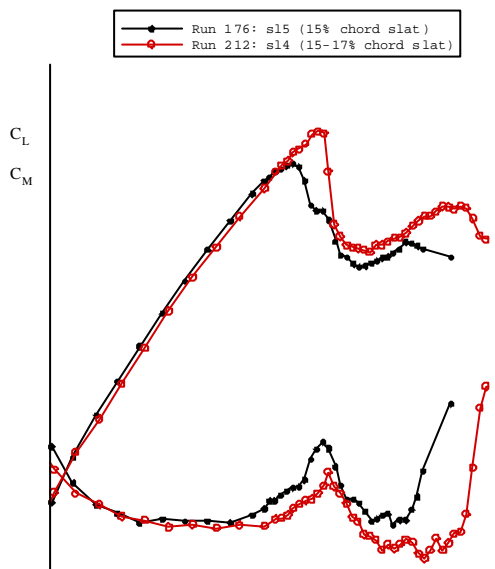

Figure 18: Effect of extending the slat chord at the wing tip from 15%c to 17%c on CRJ-700 tail-off configuration; Mach 0.20 Rec=6.5 Million. Flaps 45 degrees, slats 25 degrees

Figure 19 shows the effect on C_{Lmax} of varying the Reynolds number at Mach 0.2 on the final aircraft configuration. The variation is seen to be larger on the configuration with retracted slats and much smaller when the slats are deployed. The results showed that the data obtained at a reference chord Reynolds number of 6.5 million was a good basis for predicting full aircraft behavior.

The wind tunnel test lead to the selection of 25 degrees landing slats and 20 to 22 degrees take-off slats. Given the lower accuracy in the drag axis of the half-model test, a decision was made

to leave the final selection of the take-off slat angle to the flight test phase.
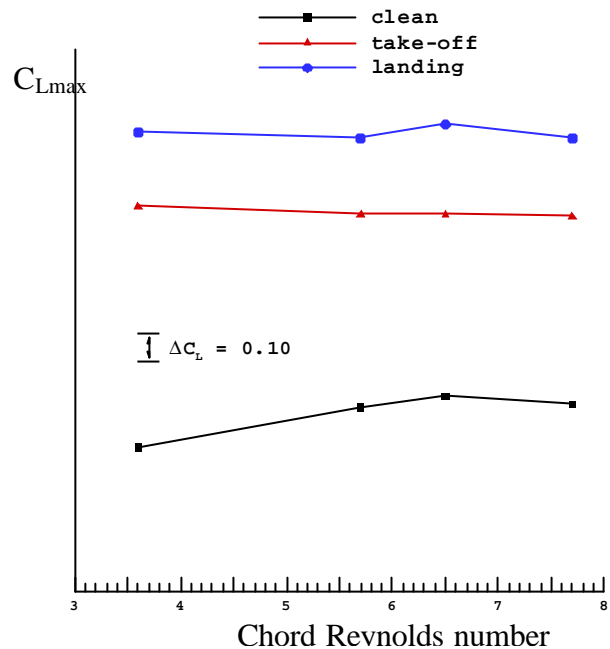

Figure 19: Effect of Reynolds number on various configurations of the CRJ-700; Mach 0.20.

6 Flight Testing

The CRJ-700 aircraft first flew on May 27, 1999 (Figure 20). The aircraft obtained Transport Canada certification on December 22, 2000. The aircraft obtained subsequently European JAA certification in January 2001 and the American FAA certified the airplane in February 2001. The aircraft entered revenue passenger service on February 2001. The high-lift configuration was ultimately validated during an extensive flight test program.

Figure 20: The CRJ-700 prototype aircraft #10001 on its maiden flight.

The aircraft is fitted with a stall protection system including a stick shaker for stall warning and a stick pusher for stall recovery. The stick pusher activates ahead of natural stall for the clean configuration and post-natural stall for all configurations with the slats deployed. Handling stall tests demonstrated compliance with all stall characteristics requirements. These included straight and turning stalls at 1 kt/sec deceleration, with power on and off, with spoilers retracted and extended and with and without lateral center of gravity imbalance. Dynamic stall entries at 3 kt/sec were also demonstrated. Figure 21 shows lift curves from the IAR 5-ft wind tunnel test, trimmed for the most forward centre of gravity, compared to equivalent data from performance flight tests. This figure shows good correlation for all flap angles. For take-off configurations requiring good climb gradient, a slat angle of 20 degrees was finally selected.
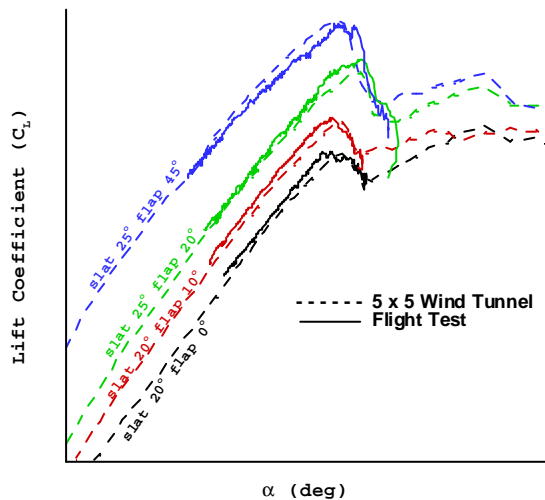

Figure 21: Comparison of trimmed lift curves from the IAR 5-ft wind tunnel test with flight test data.

7 Conclusions

The geometry and deployment schedule of the CRJ-700 flaps and slats were developed using CFD methods. The predicted characteristics of the aircraft were verified in low speed wind tunnel tests conducted with a full model at low Reynolds number and a half-model at high Reynolds number. There was good correlation between the results of the two models, except

for the pitching moments. Tailplane angles to trim and drag of high-lift configurations were therefore taken from the full-model tests with appropriate corrections for scale. Flight test data indicated that the results of half-model tests in the IAR 5ft x 5ft wind tunnel at 6.5-Million chord Reynolds number provide accurate estimates of the aircraft characteristics including C_{Lmax}. A similar conclusion was reached previously with the Global Express.

References

[1] Cebeci, T., Besnard, E. and Messie, S. "A Stability / Transition Interactive Boundary Layer Approach to Multi-Element Wings at High Lift". AIAA Paper 94-0292 (1994).

[2] Drela, M. "Newton Solution of Coupled Viscous/Inviscid Multi-Element Airfoil Flows". AIAA Paper 90-1470 (1970).

[3] Mavriplis, D.J. and Jameson, A. "Multigrid Solution of the Navier-Stokes Equations on Triangular Meshes". *AIAA Journal*, vol. 28, no. 8, pp. 1415-1425 (1990).

[4] Langlois, M., Kho, C., Kafyeke F., Mokhtarian, F.and Jones, D. "Investigation of a Multi-Element Airfoil High-Lift Characteristics at High Reynolds Numbers", *Proc. 8th CASI Aerodynamics Symposium*, Toronto, April 2001.

[5] Valarezo, W.O. and Chin, V.D. "Maximum Lift Prediction for Multielement Wings". AIAA-92-0401.

[6] Brown, D. "Information for Users of the National Research Council's f'x5' Blowndown Wind Tunnel at the National Aeronautical Establishment". LTR-HA-6. National Research Council Canada. September 1977.

[7] Mokry, M. "Subsonic Wall Interference Corrections for Half-Model Test Section Using Sparse Wall Pressure Data", NAE Aeronautical Report LT-616, 1985.